JOC The Journal of Organic Chemistry

Article

pubs.acs.org/joc

Computational Mechanistic Study of the Julia–Kocieński Reaction

Laura Legnani,* Alessio Porta, Pierluigi Caramella, Lucio Toma, Giuseppe Zanoni, and Giovanni Vidari*

Sezione di Chimica Organica, Dipartimento di Chimica, Università di Pavia, Via Taramelli 12, 27100 Pavia, Italy

Supporting Information

ABSTRACT: This paper describes the first detailed computational mechanistic study of the Julia–Kocieński olefination between acetaldehyde (**1**) and ethyl 1-phenyl-1*H*-tetrazol-5-yl sulfone (**2**), considered a paradigmatic example of the reaction between unsubstituted alkyl PT sulfones and linear aliphatic aldehydes. The theoretical study was performed within the density functional approach through calculations at the B3LYP/6-311+G(d,p) level for all atoms except sulfur for which the 6-311+G(2df,p) basis set was used. All the different intermediates and transition states encountered along the reaction pathways leading to final *E* and *Z* olefins have been located and the relative energies calculated, both for the reactions with potassium- and lithium-metalated sulfones, in THF and toluene, respectively. We have essentially confirmed the complex multistep mechanistic manifold proposed by others; however, the formation of a spirocyclic intermediate in the Smiles rearrangement was excluded. Instead, we found that this step involves a concerted, though asynchronous, mechanism. Moreover, our calculations nicely fit with the diastereoselectivities observed experimentally for potassium- and lithium-metalated sulfones, in THF and toluene, respectively.

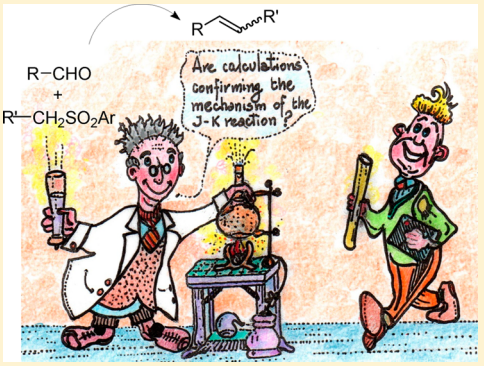

INTRODUCTION

The total synthesis of complex natural product molecules often requires the use of olefination reactions capable of joining together highly functionalized fragments to form alkene double bonds in highly regio- and stereoselective fashion. In addition, starting products must be easily obtainable and, ideally, the reaction should be atom economical and produce nontoxic products. No single method developed so far provides a universal solution to these problems.[1] Direct olefinations of carbonyl compounds probably still remain the most generally applicable methods.[1] They include, among others, the very well-known Wittig reaction, the Horner–Wittig and Horner–Wadsworth–Emmons (HWE) variants, and the Peterson, Johnson, and Julia olefinations.[2] The last one has gained a great popularity in the last decades, because of different generally applicable methods for incorporating sulfone moieties into synthetic fragments which then smoothly react with counterpart carbonyl compounds. The absence of toxicity of the sulfur derivatives and the usually high and predictable regio- and stereoselectivity of formed olefins are additional important features of this methodology. For these characteristics and the operationally simple procedures, the classical Julia reaction and the modified variants have successfully been used in the synthesis of a great number of different biologically active natural product molecules.[3] The original classical Julia olefination, discovered by Marc Julia, also known as the Julia–Lythgoe olefination,[4] consists of a multistep sequence comprising the nucleophilic attack of an α-metalated aromatic sulfone to an aldehyde affording a β-hydroxy sulfone, the conversion of the hydroxyl group to a better leaving group, typically an acyloxy or a sulfonate group, and the final reductive elimination as an olefin-forming step. This original procedure was later significantly improved by the so-called *one-pot* olefination protocol, at first developed by Sylvestre Julia and further by Kocieński, which is commonly known as the Julia–Kocieński (J-K) reaction.[3f,5] Actually, these variants encompass the need for the functionalization step; instead, olefins are directly prepared in one pot, under mild reaction conditions, from carbonyl compounds and benzothiazol-2-yl sulfones (BT sulfones) or 1-phenyl-1*H*-tetrazol-5-yl sulfones (PT sulfones) or other heteroaryl alkyl sulfones, upon the presumed Smiles rearrangement of an intermediate alkoxide.[3c,f] Moreover, there are fewer problems with scale-up than with the classical variant, and the *E*/*Z*-selectivity can be controlled to some extent by varying the sulfonyl group, the carbonyl component, the solvent polarity, and the counterion of the base.

The commonly accepted mechanistic pathways of the J-K reaction leading to the *E*-olefin (A) or the *Z*-olefin (B) are depicted in Scheme 1[3c,e,f,6] for the reaction between acetaldehyde and ethyl PT sulfone. They comprise four main steps; (i) the addition of a metalated PT sulfone to an aldehyde to give alkoxides **3E** (anti) or **3Z** (syn); (ii) the Smiles rearrangement of the folded conformations **3Eg** and **3Zg**, to give the cyclic Smiles intermediates **4E** and **4Z**, respectively, which undergo cleavage to the sulfinates **5Eg** and **5Zg**, respectively; (iii) the conformational change of the conformers **5Eg** and **5Zg**, resulting from the Smiles rearrangement, into geometries **5Ea** and **5Za**, respectively, having antiperiplanar-oriented sulfinate and OPT groups; (iv) the antiperiplanar β-

Received: January 3, 2015
Published: February 16, 2015

DOI: 10.1021/acs.joc.5b00008
J. Org. Chem. 2015, 80, 3092–3100

Scheme 1. Suggested Mechanistic Pathways A and B of the Julia–Kocieński Reaction, Leading to (*E*)-But-2-ene and (*Z*)-But-2-ene,[3c] Respectively[a]

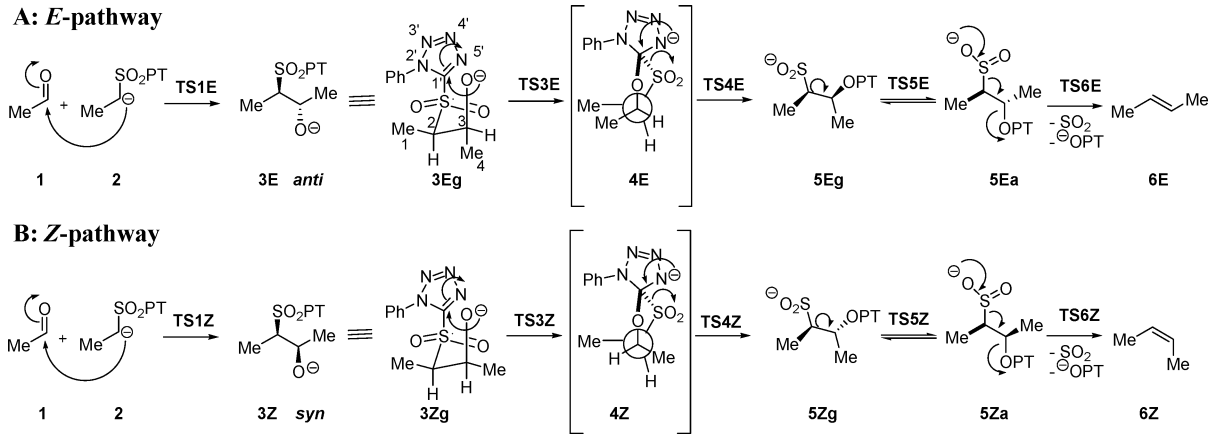

[a]The syn and anti notations indicate the relative stereochemistry of the sulfonyl and alkoxy substituents in the adducts, while the a and g symbols denote their antiperiplanar and gauche orientations, respectively. The counterion of anionic species is omitted in the scheme for the sake of clarity.

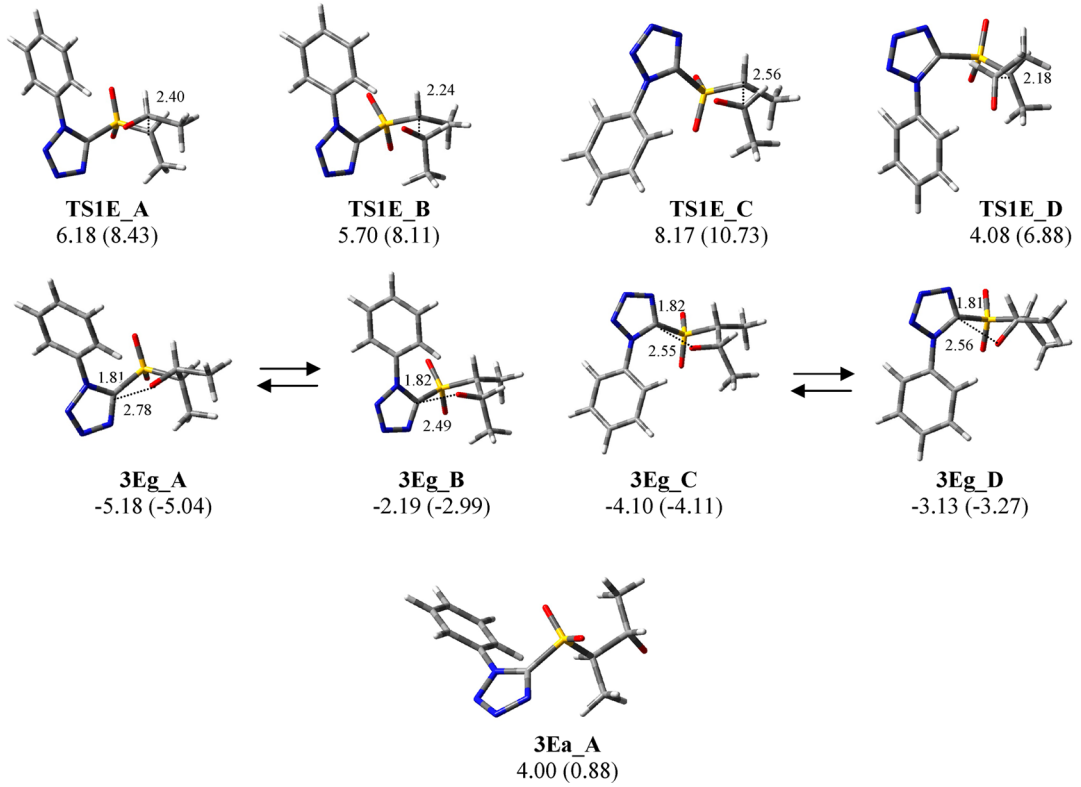

Figure 1. Three-dimensional plots of the possible conformers of **TS1E** and intermediate **3E** in the *E* pathway of the Julia–Kocieński reaction of acetaldehyde with potassium-metalated ethyl 1-phenyl-1*H*-tetrazol-5-yl sulfone in THF. The corresponding relative electronic energies (kcal/mol) in vacuo and in solvent (in parentheses), with respect to the isolated reacting species, are reported. Bond distances (Å) are indicated on the 3D plots.

elimination of sulfur dioxide and the heterocyclic moiety through the transition states **TS6E** and **TS6Z** to deliver olefin **6E** and **6Z**, respectively.

In the case of aliphatic PT sulfones, the first step has been demonstrated experimentally to be irreversible;[3f] and the final olefin ratio is then considered to be determined by the initial **3E**/**3Z** ratio. Pairing of polar and strongly coordinating solvent with a large counterion of metalated sulfones, such as a potassium cation, enhances the stereoselectivity in favor of the *E*-olefin. In contrast, in less polar and coordinating solvents, such as in toluene, the amount of the *Z*-olefin increases significantly, thus dramatically decreasing the reaction stereoselectivity.[3c,7] This effect is further enhanced when lithium is the counterion of metalated sulfones.

To the best of our knowledge, this complex multistep mechanistic manifold has never been the object of in-depth computational studies aimed at confirming the proposed different steps by locating the different intermediates and transition states (TSs) encountered along the reaction pathways leading to final olefins.[8] Besides confirming the hypothesized mechanism, we intended to shed some light upon the dependence of the reaction stereoselectivity on the type of

DOI: 10.1021/acs.joc.5b00008
J. Org. Chem. 2015, 80, 3092–3100

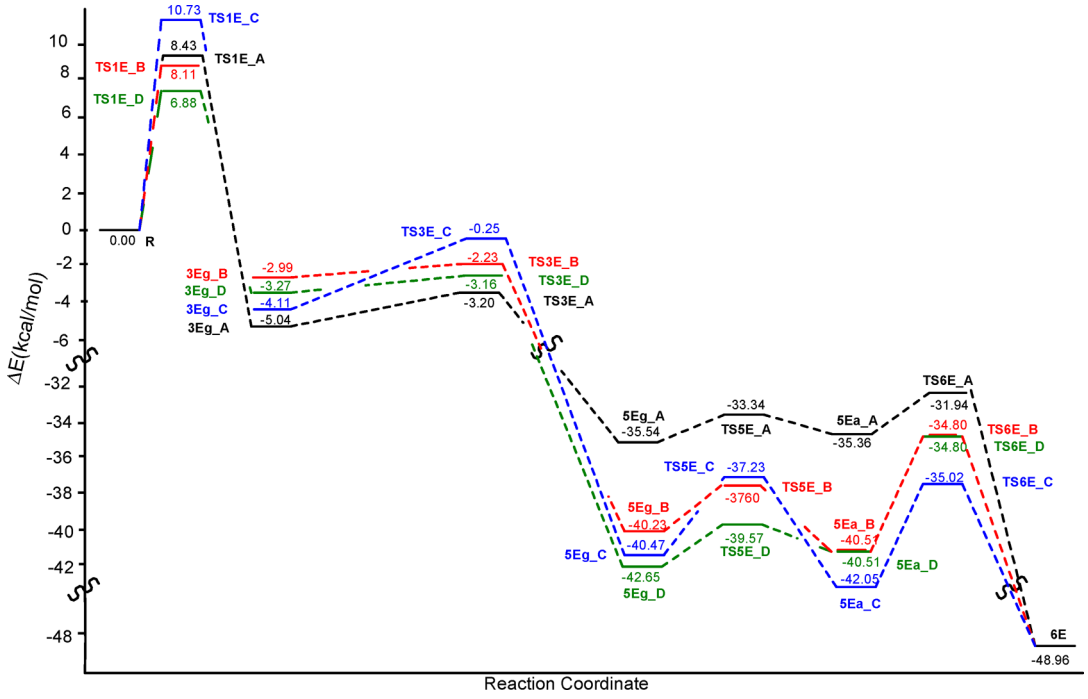

Figure 2. Energy profiles A (black), B (red), C (blue), and D (green) for the *E* pathway of the Julia–Kocieński reaction of acetaldehyde with potassium-metalated ethyl 1-phenyl-1 *H*-tetrazol-5-yl sulfone in THF.

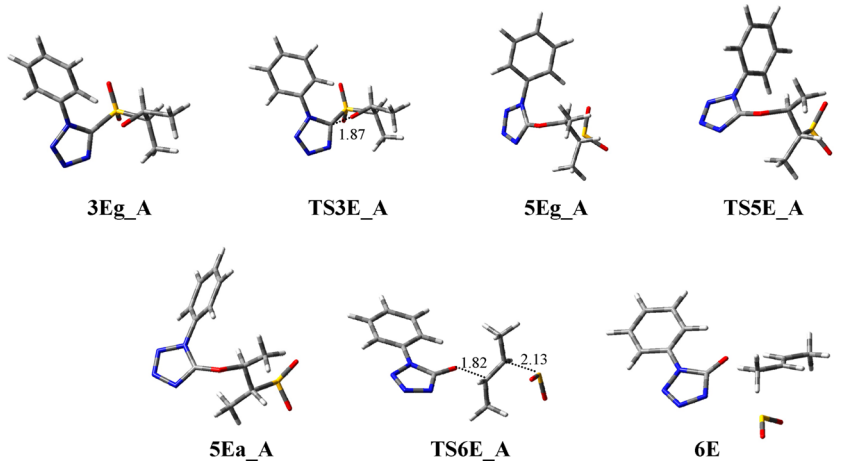

Figure 3. Julia–Kocieński reaction of acetaldehyde with potassium-metalated ethyl 1-phenyl-1 *H*-tetrazol-5-yl sulfone in THF: 3D plots of calculated intermediates and TSs in the A profile of the *E* pathway. Bond distances (Å) are reported in the 3D plots.

metal counterion and the solvent polarity. To this aim, the alternative reaction pathways leading to *E*- and *Z*-olefins were considered, starting from the addition to aldehyde of either potassium-metalated sulfone in THF or lithium-metalated sulfone in toluene.

Here we report a detailed computational mechanistic study of the J-K reaction between acetaldehyde (**1**) and ethyl 1-phenyl-1*H*-tetrazol-5-yl sulfone (**2**), which we considered a paradigmatic example of the reaction between unsubstituted alkyl PT sulfones and linear aliphatic aldehydes.

RESULTS AND DISCUSSION

Modeling of the Julia–Kocieński *E* Pathway with Potassium-Metalated Sulfone 2 in THF. Our computational study started by modeling the J-K reaction under the conditions highly favoring the formation of *E*-olefins. Experimentally, among the solvents and bases tested for the reaction between aliphatic sulfones and aliphatic aldehydes, pairing of a base having potassium as the counterion, usually KHMDS, and 1,2-dimethoxyethane (DME) as the solvent, afforded *E*-olefins with remarkable selectivity in all cases studied. It has been suggested that, under this condition, the big cation K^+ is largely coordinated by the polar solvent, favoring a dissociated carbanion, which, in the first step of the reaction, would afford anti adduct through an open transition state, that would eventually lead to the *E*-olefin.[3c] In our studies, among the solvents implemented in Gaussian, tetrahydrofuran (THF) was selected for the modeling, since it was considered the most similar to DME, as a polar coordinating ether solvent. Moreover, K^+ was selected as the base counterion, and the anionic species were thus considered, on first approximation, completely dissociated from the cation.

DOI: 10.1021/acs.joc.5b00008
J. Org. Chem. 2015, 80, 3092–3100

The geometry of isolated reacting species, i.e., acetaldehyde **1** and the α-anion of the PT sulfone **2**, were at first optimized; subsequently, the modeling study examined the first step, namely the addition of **2** to **1** to give the anti adduct (2*R**,3*S**)-**3E**.

All the possible minimum energy conformers of the adduct **3E** were located, but only the four geometries **3Eg_A−D** (Figure 1), corresponding to the gauche conformer **3Eg** (Scheme 1), having the anionic oxygen atom spatially close to the tetrazole ring, were significantly populated. The other conformers were less stable by about 10 kcal/mol in vacuo, and 6−8 kcal/mol in THF. In particular, a geometry of type **3Ea_A** (Figure 1), in which the dipoles associated with the carbonyl and the sulfonyl groups are anti-oriented, was calculated to be 9.2 kcal/mol in vacuo and 5.9 kcal/mol in THF higher in energy than the most stable conformer **3Eg_A**.

In each of the four transition states **TS1E_A−D** (Figure 1), collapsing to **3Eg_A−D**, respectively, the two dipoles were gauche-oriented, and the least sterically crowded transition state **TS1E_D** was found to be preferred by about 1−4 kcal/mol over the other three pathways. However, it is worth pointing out that the most stable conformer of **3E** was calculated to be **3Eg_A**, deriving from a TS about 2 kcal/mol less stable than that of **TS1E_D**.

Considering the short distance between the anionic oxygen atom and the tetrazole carbon atom (2.49−2.78 Å) in conformers **3Eg_A−D**, a quasi-five-membered ring could be envisioned, showing different puckering modes and orientations of the substituents. The phenyl group of the PT moiety was trans-oriented with respect to the adjacent methyl groups in **3Eg_A** and **3Eg_B** while positioned in cis fashion in **3Eg_C** and **3Eg_D**.

Each conformation **3Eg_A−D** of intermediate **3E** was then the starting point of four reaction pathways converging to (*E*)-but-2-ene, whose energy profiles were all located (Figure 2). As a typical example, the 3D plots of the calculated TSs and intermediates for the different steps of the A profile are reported in Figure 3. The graphic clearly shows that after the initial formation of adduct **3E**, the reaction readily evolves through the following steps to the final product. Noteworthy, the calculated activation energy barrier of 2−3 kcal/mol for the interconversion between conformations **3Eg_A** and **3Eg_B**, and between **3Eg_C** and **3Eg_D**, through rotation around the single bond C(2)−C(3), was comparable with the activation energies of the different reaction steps. Therefore, due to the rapid conformer interconversion, the A pathway was indistinguishable from B, and C was indistinguishable from D. On the contrary, the conversion of **3Eg_A** to **3Eg_D**, and **3Eg_B** to **3Eg_C**, via rotation around the single bond C(1′)−S, was much more sluggish, due to an energy barrier of about 17 and 13 kcal/mol, respectively.

In the suggested mechanism of the J-K reaction,[3c,f,6] intermediate **3Eg** is converted to sulfinate **5Eg** via an intramolecular nucleophilic aromatic substitution, the so-called Smiles reaction.[9] It has been proposed that such rearrangement would occur through the so-called Smiles intermediate **4E** (Scheme 1), even if evidence for both a stepwise and a concerted mechanism exist in literature for the Smiles reaction.[9] Both the mechanisms were considered in our study; however, the search of an energy minimum along the reaction coordinate corresponding to the spirocyclic intermediate **4E** met with no success. In fact, every starting geometry corresponding to the predictable features of the supposed Smiles intermediate collapsed either to the alkoxide **3Eg** or to the sulfinate **5Eg**, while the cyclic structure **4E** was not located as an energy minimum. In striking contrast, the geometry **TS3E** was located as a low energy transition state.

The IRC analysis (Figure 4), starting from **TS3E_A**, was performed in both the forward and the backward directions and

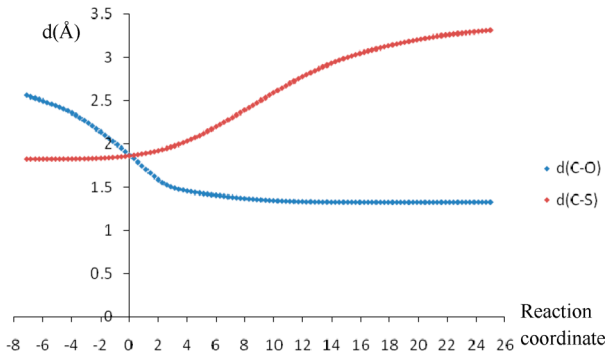

Figure 4. Length (Å) of the forming C−O and breaking C−S bonds [*d*(C−O) and *d*(C−S), respectively] at the forward (positive) and backward (negative) points in the IRC analysis, starting from **TS3E_A** (point 0), of the conversion of intermediate **3Eg_A** to **5Eg_A**.

confirmed this geometry for the transition state of the conversion of adduct **3Eg_A** to intermediate **5Eg_A**. Moreover, the accurate examination of the bond forming and breaking timing indicated that they occurred in a concerted, though asynchronous, fashion. Actually, the length of 1.86 Å for the partial C−S bond in **TS3E_A** almost corresponded to the intact single bond (1.81 Å) in **3Eg_A**, whereas the length of 1.87 Å for the partial C−O bond in **TS3E_A** indicated that the formation of this new bond had already progressed significantly. In conclusion, the conversion of **3Eg** to **5Eg** did not involve the formation of an intermediate, like the Smiles spirocyclic derivative **4E**; on the contrary, the process corresponded to a fast intramolecular nucleophilic substitution occurring in a concerted, though asynchronous, manner.

In this context, we examined the charge distribution in **3Eg_A**, **TS3E_A**, and **5Eg_A** (Figure 5), in particular, the distribution of the negative charge. In fact, the examination of the stepwise mechanism proposed for the Smiles rearrangement (Scheme 1) clearly shows that a net transfer of negative charge should occur from the alkoxide oxygen atom in **3Eg_A** to the N(5′) atom of the tetrazole ring in the Smiles intermediate **4E**. In striking contrast, instead, our data showed that in the transition state **TS3E_A** most of the negative charge is still retained by the alkoxide oxygen atom attacking the positively charged carbon of the tetrazole ring, while it is transferred to N(5′) only marginally. Moreover, while the TS collapses to the final product **5Eg_A**, the negative charge on the oxygen is mostly transferred onto the positively charged sulfur atom of the sulfonyl group, which thus becomes a good leaving group and finally detaches as a sulfinate. Thus, the ability of the leaving group in stabilizing the negative charge appears to be a crucial factor to force the Smiles reaction of intermediate **3Eg** to proceed through a concerted pathway. Similar considerations have been applied to other concerted nucleophilic displacement reactions at sp^2 trigonal carbons, including those in (aryloxy)triazines[10a] and some nucleophilic acyl substitution reactions involving excellent leaving groups.[10b−d]

DOI: 10.1021/acs.joc.5b00008
J. Org. Chem. 2015, 80, 3092−3100

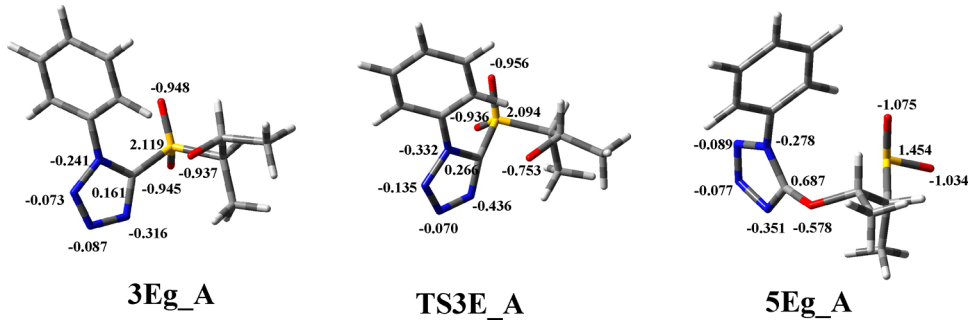

Figure 5. NBO charge distribution in **3Eg_A**, **TS3E_A**, and **5Eg_A**.

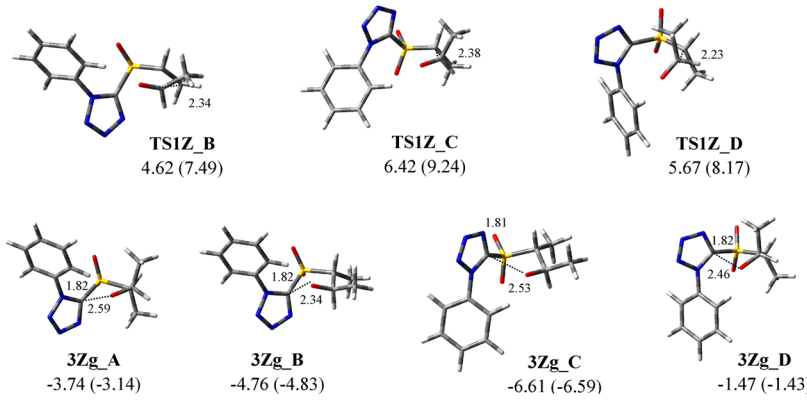

Figure 6. Three-dimensional plots of the possible conformers of **TS1Z** and intermediate **3Zg** in the *Z* pathway from potassium-metalated sulfone **2**. The corresponding relative electronic energies (kcal/mol) in vacuo and in THF (in parentheses), with respect to the isolated reacting species, are reported. Bond distances (Å) are reported in the 3D plots.

We then examined the last two steps of the *E*-olefin formation, namely: (i) the rotation of sulfinate **5Eg** around the C(2)−C(3) single bond to the antiperiplanar conformation **5Ea**, having the stereoelectronically required geometry for triggering the following *β*-elimination step; (ii) the extrusion of sulfur dioxide with concerted elimination of the PT heterocyclic moiety. The rotational energy barriers **TS5E** between **5Eg** and **5Ea** was found to be low (2−3 kcal/mol) while the antiperiplanar *β*-elimination to the *E*-olefin **6E** was estimated to take place through a slightly higher energy barrier, involving the transition state **TS6E** in which the rupture of the C−S bond was more advanced than that of the C-OPT bond.

Two alternative mechanisms for the elimination of the sulfinate and the OPT moieties from the intermediate **5Eg** to give the final olefin were also examined. In the first, the direct synperiplanar elimination of the two groups were considered, which would lead to the *cis*-olefin **6Z**. Although stereoelectronically disfavored compared to the antiperiplanar elimination, this mechanism would not require the preliminary rotation of **5Eg** around the C(2)−C(3) single bond to give **5Ea**.

The calculated energy barrier of the synperiplanar elimination was, however, calculated to be 8.7 kcal/mol *in vacuo* and 10.4 kcal/mol in THF higher than the barrier for the antiperiplanar elimination, clearly indicating that the former mechanism was an unlikely process.

The other mechanism considered for the formation of the *E*-olefin from **5Eg** was a kind of two-step E1cb-like process. Actually, we envisioned the possibility that the spontaneous departure of sulfur dioxide from **5Eg** could generate a carbanion on C(2), which would then expel the OPT group to afford the final double bond. In this event, the search for an energy barrier of this process was, however, unfruitful, and no TS was located, thus excluding also this stepwise mechanism.

Modeling of the Julia−Kocieński *Z* Pathway with Potassium-Metalated Sulfone 2 in THF. Our calculations were then extended to the alternative pathway of the reaction between acetaldehyde **1** and potassium-metalated PT sulfone **2** in THF, leading to the less favored *Z*-olefin **6Z**. At first, the addition step giving the intermediate **3Z** was modeled. Only the specific arrangement represented as **3Zg**, with the anionic oxygen facing the tetrazole ring, was significantly populated, while the other geometries were less stable by 7−15 kcal/mol in vacuo and 6−9 kcal/mol in THF. Similarly to intermediate **3Eg** in the *E* pathway, alkoxide **3Zg** existed in four different conformations (**3Zg_A**−**D**) (Figure 6). Due to the unfavorable gauche interactions between one methyl group and the tetrazole ring, conformations **3Zg_A** and **3Zg_D**, though having the two methyls in an antiperiplanar orientation, were less stable than the conformations **B** and **C** having gauche methyl groups. Moreover, **3Zg_A** quickly converted to **3Zg_B** through a low energy barrier of about 0.60 kcal/mol, both in vacuo and in THF, while the conversion of **3Zg_D** to **3Zg_C** was even faster.

Noteworthy, adducts **B** and **C** and the corresponding TSs showed an inverted stability. In fact, although **3Zg_C** was the most stable conformer of **3Zg**, the corresponding transition state **TS1Z_C** was 1.80 kcal/mol in vacuo and 1.75 kcal/mol in THF higher in energy than the lowest energy transition state **TS1Z_B**, collapsing to **3Zg_B**. Attempts to locate **TS1Z_A** failed, while a relaxed potential energy surface scan of the cleavage of the C−C bond of **3Zg_A** afforded **TS1Z_B**.

DOI: 10.1021/acs.joc.5b00008
J. Org. Chem. 2015, 80, 3092−3100

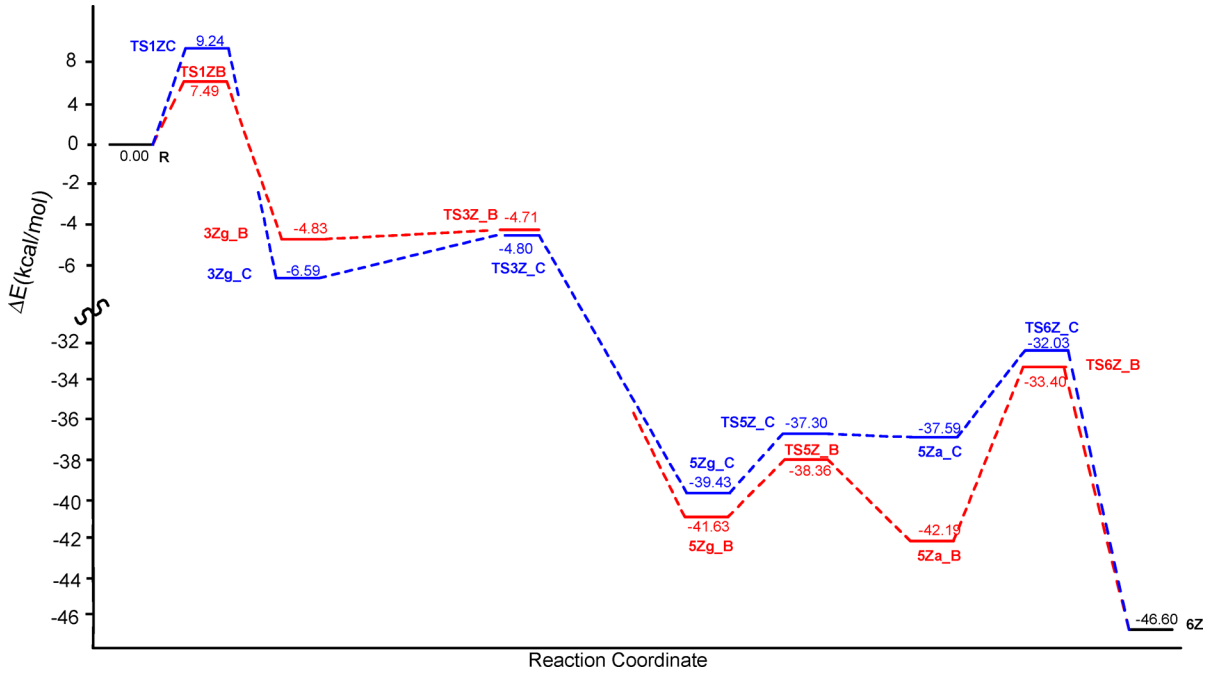

Figure 7. Energy profiles B (red), and C (blue) for the *Z* pathway of the Julia–Kocieński reaction of acetaldehyde with potassium-metalated ethyl 1-phenyl-1*H*-tetrazol-5-yl sulfone in THF.

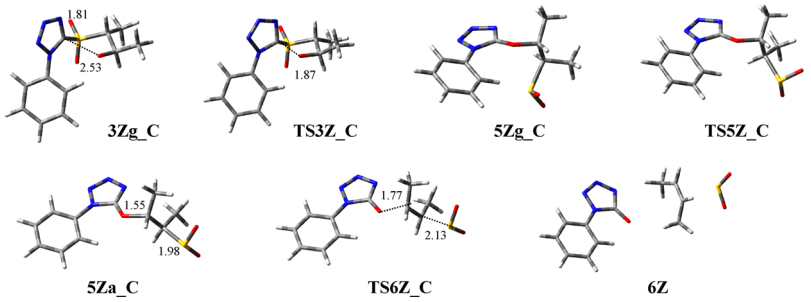

Figure 8. Three-dimensional plots of the intermediates and the transition states in the *Z* pathway of the Julia–Kocieński reaction proceeding from the conformer **3Zg_C** of adduct **3Zg**. Bond distances (Å) are reported in the 3D plots.

The reaction then proceeded from **3Zg_B** and **3Zg_C** to the final product (*Z*)-but-2-ene through intermediates and TS analogous to the *E*-pathway affording (*E*)-but-2-ene (Figure 7). In Figure 8 the 3D plots of the transition states and intermediates in the reaction pathway proceeding from **3Zg_C** are reported, as an indicative example.

The **3Zg_C** adduct was then rapidly converted to sulfinate **5Zg_C** via the transition state **TS3Z** in which the formation of the new C–O bond (1.87 Å) proceeded in a concerted, however asynchronous, fashion with the breaking of the C–S bond (1.84 Å). Noteworthy, as observed for the *E* pathway, the existence of the presumed spirocyclic Smiles structure **4Z** was not detected, likely due to the same electronic factors discussed before. Subsequently, a rapid rotation around the C(2)–C(3) single bond allowed the sulfinate **5Zg_C** to assume the conformation **5Za_C**, in which the two methyl groups were gauche-oriented. In the final step of the pathway, the concomitant antiperiplanar β-elimination of the PTO moiety and sulfur dioxide occurred via the transition state **TS6Z**, affording the *Z*-olefin **6Z**.

According to the mechanistic manifold for irreversible J-K reactions between aldehydes and the α-anion of PT sulfones, such as **1** and **2**, the final olefin ratio is determined by the relative rate of formation of adducts **3E** and **3Z** in the first step.[3c] Our calculations predicted an energy difference of 0.54 kcal/mol in vacuo and 0.61 kcal/mol in THF for the transition states **TS1E_D** and **TS1Z_B** in the *E* and *Z* pathways, respectively (Figures 2 and 7), corresponding to an *E*/*Z*-selectivity = 75:25 in vacuo, and 78:22 in THF at −78 °C. These values were nicely comparable with the *E*/*Z* ratio = 86:14 determined for the reaction between hexanal and potassium-metalated pentyl phenyltetrazolyl sulfone at −78 °C, considered as the reference reaction.[7]

Modeling of the Julia–Kocieński *E* and *Z* Pathways with Lithium-Metalated Sulfone 2 in Toluene. A decrease in the *E*/*Z* olefin ratio has been observed experimentally for the Julia–Kocieński reactions as the counterion of metalated sulfones is changed from K^+ to Li^+ in an apolar, poorly coordinating solvent, for example toluene.[3c] It has been suggested that this significant drop in the diastereoselectivity would be due to an increase of populated chelated transition states in the first step of the J-K reaction,[3c] that would be largely favored by small cations in noncoordinating apolar solvents. The chelation effect would lead, preferentially, to **3Z**-like syn adducts instead of **3E**-like anti ones, resulting, at the

DOI: 10.1021/acs.joc.5b00008
J. Org. Chem. 2015, 80, 3092–3100

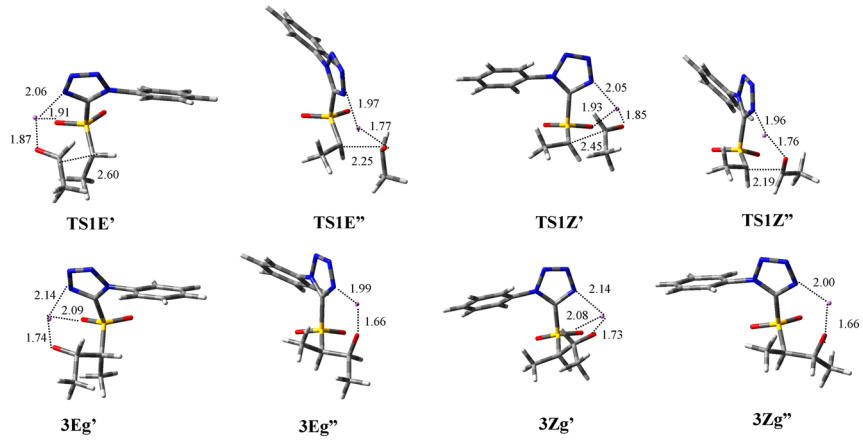

Figure 9. Three-dimensional plots of the intermediates and the transition states having a di- and a tricoordinated lithium ion in the *Z* and *E* pathways of the Julia–Kocieński reaction with lithium-metalated sulfone **2** in toluene. Bond distances (Å) are reported in the 3D plots.

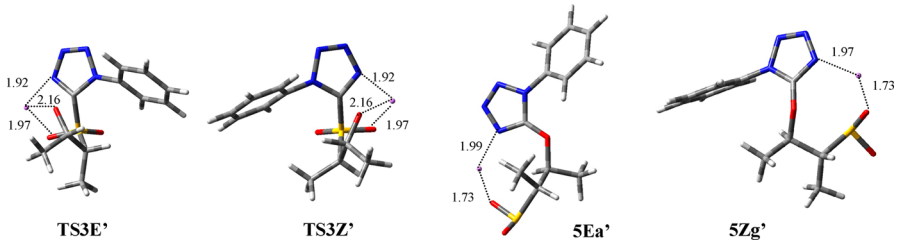

Figure 10. Three-dimensional plots of **TS3E′**, **TS3Z′**, and their sulfinates **5** coordinated to lithium ion in the *E* and *Z* pathways of the Julia–Kocieński reaction. Distances between lithium and coordinated atoms (Å) are reported in the 3D plots.

end of the reaction pathway, in an increasing proportion of the *Z*-olefin.

To test this hypothesis, at first we modeled the transition states leading to lithium-chelated syn and anti adducts for the reaction between aldehyde **1** and lithium-metalated sulfone **2** in toluene at −78 °C, by introducing the lithium ion in the calculations.[11] Two types of transition states were found for both the *E* and Z pathways, in which lithium was tricoordinated and dicoordinated, respectively. Figure 9 shows two representative TSs for the syn addition, **TS1Z′** and **TS1Z″**, and two for the anti addition, **TS1E′** and **TS1E″**. In **TS1Z′** and **TS1E′** the cation was chelated to the N(3′) of the tetrazole ring, the alkoxy anion, and one oxygen of the sulfone moiety, while in **TS1Z″** and **TS1E″** the lithium was only chelated to N(3′) and the alkoxy anion (Figure 9). The energy values (see Supporting Information) allowed the calculation of energy barriers corresponding to a final ratio of (*E*)- and (*Z*)-but-2-ene of 10:90 for the tricoordinated lithium pathway and 51:49 for the less favored dicoordinated one. Thus, the modeling clearly indicated the major role played by the lithium coordination in apolar solvents in favoring the formation of *Z*-olefins in the J-K reaction, though the calculated *E*/*Z* ratio did not exactly reproduce the stereoselectivity found experimentally,[7] due to an overestimated proportion of the *Z*-olefin. Besides an incomplete modeling accuracy, this discrepancy may be simply due to the presence of competing transition states, in which anionic species are loosely coordinated to lithium. Actually, these transition states would resemble those modeled with potassium as the counterion (see above), which would preferentially afford (*E*)-but-2-ene.

The four transition states **TS1Z′**, **TS1E′**, **TS1Z″**, and **TS1E″** collapsed to the two lithium-tricoordinated adducts **3Zg′** and **3Eg′**, and the two metal-dicoordinated adducts **3Zg″** and **3Eg″**, respectively. As expected, the tricoordinated species were more stable than the corresponding dicoordinated ones.

It was then interesting to explore whether, according to the general mechanistic manifold suggested for the J-K reaction (Scheme 1),[3c,f,6] lithium-chelated intermediates would convert to the corresponding sulfinates through the corresponding Smiles intermediates. As found for the reaction pathway with potassium-metalated sulfones, modeled above, the search for an energy minimum along the reaction coordinate corresponding to spirocyclic intermediates such as **4E** and **4Z** met with no success. In fact, these cyclic structures were not located as energy minima. In striking contrast, and quite remarkably, both **3Zg′** and **3Zg″** converged to the same sulfinate **5Zg′** via a concerted asynchronous mechanism involving the same transition state **TS3Z′** (Figure 10). Analogously, in the *E* pathway, the corresponding di- and tricoordinated **3E** adducts converged to the same **5Ea′** sulfinate through an identical transition state (Figure 10). For the two TSs, in which the new C–O bond was only partially formed, similarly chelated tricoordinated structures were observed (Figure 10). Conversely, sulfinates **5Ea′** and **5Zg′**, in which the C–O bond was completely formed, existed as dicoordinated structures, having the lithium ion linked only to N(3′) and one sulfone oxygen (Figure 10).

The reaction then proceeded uneventfully from intermediates **5Ea′** and **5Zg′** to the final olefins **6E** and **6Z**, respectively, as highlighted by the energy pathways A and B depicted in Figure 11. Interestingly, in **5Ea′** the PTO and the sulfinate moieties were already positioned in the antiperiplanar orientation required for triggering the subsequent *β*-elimination step, while **5Zg′** attained such geometry through fast rotation around the single bond C(2)–C(3).

DOI: 10.1021/acs.joc.5b00008
J. Org. Chem. 2015, 80, 3092–3100

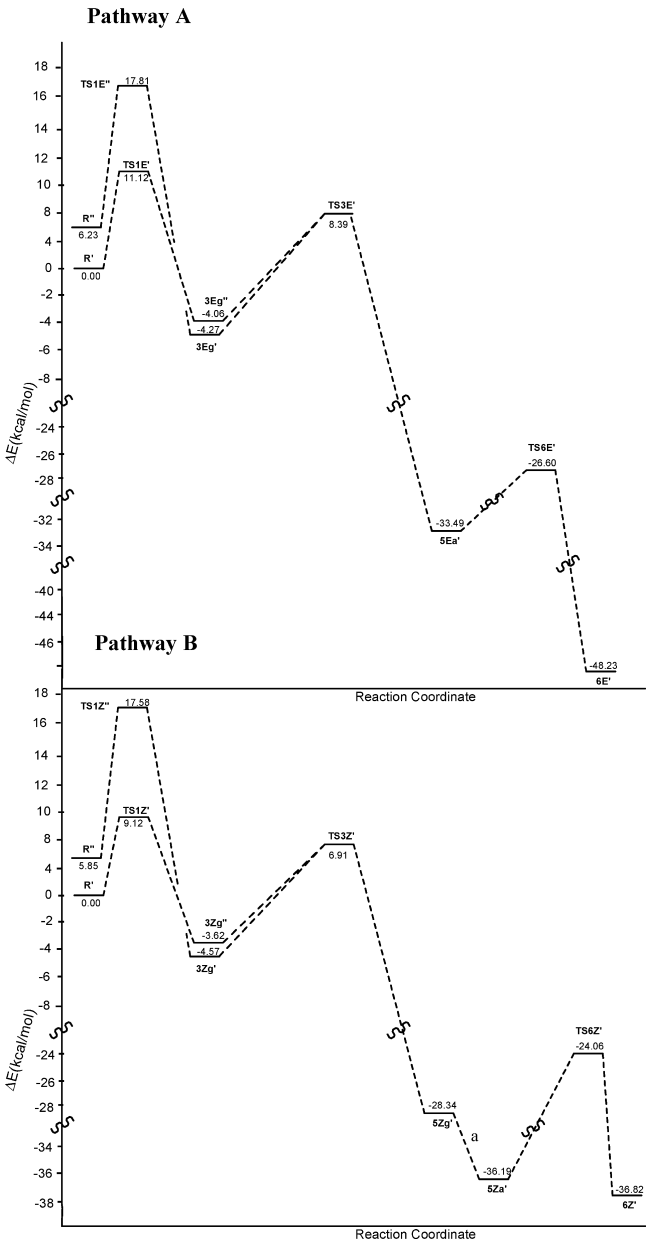

Figure 11. Energy profiles for the Julia–Kocieński reaction of acetaldehyde with lithium-metalated sulfone **2** in toluene, leading to (*E*)-but-2-ene (pathway A) and (*Z*)-but-2-ene (pathway B), respectively. [a]All attempts to locate **TS5Z**′ in pathway B failed, likely due to the rapid conversion of **5Zg**′ to **5Za**′.

CONCLUSIONS

The Julia–Kocieński reaction between heteroaryl sulfones and aldehydes is one of the most popular procedures to obtain substituted olefins with usually excellent *E*-selectivity.[2,3] In this paper we have reported the first detailed mechanistic study of the J-K reaction between acetaldehyde (**1**) and metalated ethyl 1-phenyl-1*H*-tetrazol-5-yl sulfone (**2**), which we considered a paradigmatic example of the reaction between unsubstituted alkyl PT sulfones and linear aliphatic aldehydes. The theoretical study was performed within the density functional approach through calculations at the B3LYP/6-311+G(d,p) level for all atoms except sulfur for which the 6-311+G(2df,p) basis set was used.[12] Moreover, single-point calculations by using a solvent polarizable continuum model[13] were performed to take solvent effects into account. All the different intermediates and transition states encountered along the reaction pathways leading to final (*E*)-but-2-ene and (*Z*)-but-2-ene have been located and the relative energies have been calculated, both for the reaction with potassium-metalated sulfone in THF and with lithium-metalated sulfone in toluene.

We have essentially confirmed the complex multistep mechanistic manifold proposed by others,[3c,f,6] with the remarkable exception of the formation of the intermediate Smiles spirocyclic derivatives **4E** and **4Z**. Actually, these species have been proposed as energy minimum intermediates in the conversion of the initial adducts **3E** and **3Z** to sulfinates **5E** and **5Z**, respectively.[3c,f,6] On the contrary, we found that the formation of the new C–O bond proceeded in a concerted, however, asynchronous fashion with the breaking of the C–S bond, so that the process corresponded to a fast intramolecular nucleophilic aromatic reaction proceeding in a concerted, though asynchronous, fashion. Moreover, our calculations nicely fit with the experimental data[7] showing that metal-free sulfone anions, such as those formed by metalation with a potassium base in polar and coordinating solvent, such as THF, enhances the reaction *E*-diastereoselectivity. In contrast, with lithium as sulfone anion counterion in a less polar and coordinating solvent, such as toluene, the amount of the *Z*-olefin was found to increase significantly, resulting in a dramatic decrease of the reaction stereoselectivity.

Our modeling study will now be extended to more complex substrates, including the Julia–Kocieński reactions between substituted sulfones and aldehydes. Our findings will be reported in due time.

EXPERIMENTAL SECTION

Computational Methods. All the calculations were carried out using the GAUSSIAN09 program package.[14] All the structures of reactants, transition states, intermediates, and products were optimized in the gas phase at the B3LYP/6-311+G(2df,p) level for the S atom and 6-311+G(d,p) level[12] for the other atoms to correctly describe geometries and electronic properties of compounds containing a sulfur atom, belonging to the third period. The reaction pathways were confirmed by IRC analyses performed at the same level as above. Vibrational frequencies were computed at the same level of theory to define the optimized structures as minima or transition states, which present an imaginary frequency corresponding to the forming bonds. Thermodynamics at 298.15 K allowed the enthalpies and the Gibbs free energies to be calculated. The solvent effects were considered by single-point calculations, at the same level as above, on the gas-phase optimized geometries, using a self-consistent reaction field (SCRF) method, based on the polarizable continuum model (PCM).[13] NBO analysis was performed at the same level of calculations.[15]

ASSOCIATED CONTENT

Supporting Information

B3LYP/6-311+G(d,p) (for C, H, O, N, Li atoms) and 6-311+G(2df,p) level (for S atom) energies and cartesian coordinates of all intermediates and transition states along the reaction pathways. This material is available free of charge via the Internet at http://pubs.acs.org.

AUTHOR INFORMATION

Corresponding Authors

*Tel: (+39) 0382987311. Fax: (+39) 0382987323. E-mail: laura.legnani@unipv.it.
*Tel: (+39) 0382987322. Fax: (+39) 0382987323. E-mail: vidari@unipv.it.

DOI: 10.1021/acs.joc.5b00008
J. Org. Chem. 2015, 80, 3092–3100

Notes

The authors declare no competing financial interest.

■ ACKNOWLEDGMENTS

Prodest Scarl is warmly thanked for a postdoctoral fellowship to L.L. The Italian MIUR is acknowledged for financial support (funds PRIN 2010-2011).

■ REFERENCES

(1) (a) *Preparation of Alkenes: A Practical Approach*; Williams, J. M. J., Ed.; Oxford University Press: Oxford, 1996. (b) Kelly, S. E. Alkene Synthesis. In *Comprehensive Organic Synthesis*; Trost, B. M., Fleming, I., Eds.; Pergamon: Oxford, 1991, Vol. *1*, pp 729−817.

(2) (a) Kürti, L.; Czakó, B. *Strategic Applications of Named Reactions in Organic Synthesis*; Elsevier Academic Press: Burlington, MA, 2005. (b) Johnson, C. R.; Shanklin, J. R.; Kirchhoff, R. A. *J. Am. Chem. Soc.* **1973**, *95*, 6462−6463.

(3) (a) Chatterjee, B.; Bera, S.; Mondal, D. *Tetrahedron: Asymmetry* **2014**, *25*, 1−55. (b) Lorente, A.; Albericio, F.; Álvarez, M. *J. Org. Chem.* **2014**, *79*, 10648−10654. (c) Aïssa, C. *Eur. J. Org. Chem.* **2009**, 1831−1844. (d) Zanoni, G.; Brunoldi, E. M.; Porta, A.; Vidari, G. *J. Org. Chem.* **2007**, *72*, 9698−9703. (e) Plesniak, K.; Zarecki, A.; Wicha, J. *Top. Curr. Chem.* **2007**, *275*, 163−250. (f) Blakemore, P. R. *J. Chem. Soc., Perkin Trans 1* **2002**, 2563−2585. (g) Nájera, C.; Yus, M. *Tetrahedron* **1999**, *55*, 10547−10658.

(4) Julia, M.; Paris, J.-M. *Tetrahedron Lett.* **1973**, *14*, 4833−4836.

(5) Baudin, J. B.; Hareau, G.; Julia, S. A.; Ruel, O. *Tetrahedron Lett.* **1991**, *32*, 1175−1178.

(6) Baudin, J. B.; Hareau, G.; Julia, S. A.; Lorne, R.; Ruel, O. *Bull. Soc. Chim. Fr.* **1993**, *130*, 856−878.

(7) Blakemore, P. R.; Cole, W. J.; Kocieński, P. J.; Morley, A. *Synlett* **1998**, 26−28.

(8) For computational mechanistic studies for the fluoro-Julia−Kocieński olefination of aldehydes with BTFP sulfones, see: Alonso, D. A.; Fuensanta, M.; Gómez-Bengoa, E.; Nájera, C. *Adv. Synth. Catal.* **2008**, *350*, 1823−1829.

(9) Truce, W. E.; Kreider, E. M.; Brand, W. W. *Org. React.* **1970**, *18*, 99−215.

(10) (a) Hunter, A.; Renfrew, M.; Rettura, D.; Taylor, J. A.; Whitmore, J. M. J.; Williams, A. *J. Am. Chem. Soc.* **1995**, *117*, 5484−5491. (b) *Concerted organic and bio-organic mechanisms*; Williams, A., CRC Press: Boca Baton, FL, 2000. (c) Williams, A. *Chem. Soc. Rev.* **1994**, *23*, 93−100. (d) Williams, A. *Acc. Chem. Res.* **1989**, *22*, 387−392.

(11) The solvation sphere of the lithium ion was not considered to simplify the computational studies.

(12) (a) Becke, A. D. *J. Chem. Phys.* **1993**, *98*, 5648−5652. (b) Lee, C.; Yang, W.; Parr, R. G. *Phys. Rev. B* **1988**, *37*, 785−789.

(13) (a) Cancés, E.; Mennucci, B.; Tomasi, J. *J. Chem. Phys.* **1997**, *107*, 3032−3042. (b) Cossi, M.; Barone, V.; Cammi, R.; Tomasi. *J. Chem. Phys. Lett.* **1996**, *255*, 327−335. (c) Barone, V.; Cossi, M.; Tomasi, J. *J. Comput. Chem.* **1998**, *19*, 404−417.

(14) Frisch, M. J.; Trucks, G. W.; Schlegel, H. B.; Scuseria, G. E.; Robb, M. A.; Cheeseman, J. R.; Scalmani, G.; Barone, V.; Mennucci, B.; Petersson, G. A.; Nakatsuji, H.; Caricato, M.; Li, X.; Hratchian, H. P.; Izmaylov, A. F.; Bloino, J.; Zheng, G.; Sonnenberg, J. L.; Hada, M.; Ehara, M.; Toyota, K.; Fukuda, R.; Hasegawa, J.; Ishida, M.; Nakajima, T.; Honda, Y.; Kitao, O.; Nakai, H.; Vreven, T.; Montgomery, J. A., Jr.; Peralta, J. E.; Ogliaro, F.; Bearpark, M.; Heyd, J. J.; Brothers, E.; Kudin, K. N.; Staroverov, V. N.; Keith, T.; Kobayashi, R.; Normand, J.; Raghavachari, K.; Rendell, A.; Burant, J. C.; Iyengar, S. S.; Tomasi, J.; Cossi, M.; Rega, N.; Millam, J. M.; Klene, M.; Knox, J. E.; Cross, J. B.; Bakken, V.; Adamo, C.; Jaramillo, J.; Gomperts, R.; Stratmann, R. E.; Yazyev, O.; Austin, A. J.; Cammi, R.; Pomelli, C.; Ochterski, J. W.; Martin, R. L.; Morokuma, K.; Zakrzewski, V. G.; Voth, G. A.; Salvador, P.; Dannenberg, J. J.; Dapprich, S.; Daniels, A. D.; Farkas, O.; Foresman, J. B.; Ortiz, J. V.; Cioslowski, J.; Fox, D. J. *Gaussian 09, Revision B.01*; Gaussian, Inc., Wallingford, CT, 2010.

(15) (a) Foster, J. P.; Weinhold, F. *J. Am. Chem. Soc.* **1980**, *102*, 7211−7218. (b) Reed, A. E.; Weinstock, R. B.; Weinhold, F. *J. Chem. Phys.* **1985**, *83*, 735−746.

DOI: 10.1021/acs.joc.5b00008
J. Org. Chem. 2015, 80, 3092−3100